Tensor RG calculations and quantum simulations near criticality

Yannick Meurice

The University of Iowa

yannick-meurice@uiowa.edu

With Alexei Bazavov, Shan-Wen Tsai, Judah Unmuth-Yockey, Li-Ping Yang, and Jin Zhang

Lattice 2016, July 26

Content of the talk

- The Tensor Renormalization Group (TRG) method
- The $O(2)$ model with a chemical potential (1+1 dimensions)
- von Neumann entanglement entropy
- Rényi entanglement entropy
- Calabrese-Cardy scaling and central charge estimates
- Can we measure the central charge using optical lattices?
- The Abelian Higgs model (1+1 dimensions)
- Probing the $O(2)$ model with weakly coupled gauge fields
- The Polyakov's loop
- Conclusions

The Tensor Renormalization Group (TRG) method

- Exact blocking (spin and gauge, PRD 88 056005)

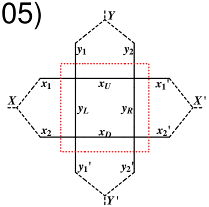

Unique feature: the blocking separates the degrees of freedom inside the block (integrated over), from those kept to communicate with the neighboring blocks. The only approximation is the truncation in the number of “states" kept.

- Applies to many lattice models: Ising model, $O(2)$ model, $O(3)$ model, $SU(2)$ principal chiral model (in any dimensions), Abelian and $SU(2)$ gauge theories (1+1 and 2+1 dimensions)
- Solution of sign problems: complex temperature (PRD 89, 016008), chemical potential (PRA 90, 063603)
- Checked with worm sampling (Chandrasekharan, Gattringer ...)
- Critical exponents of Ising (PRB 87, 064422; Kadanoff RMP 86)
- Connects easily to the Hamiltonian picture and provides spectra
- Used to design quantum simulators: $O(2)$ model (PRA 90, 063603), Abelian Higgs model (PRD 92 076003) on optical lattices

- 1+1 dimensions: phase diagram of $O(2)$ + chemical potential (PRA 90, 063603) and Entanglement entropy (PRE 93, 012138)

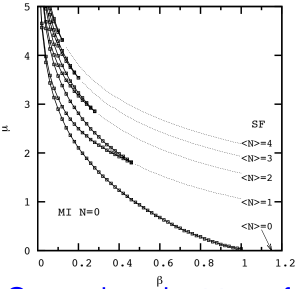

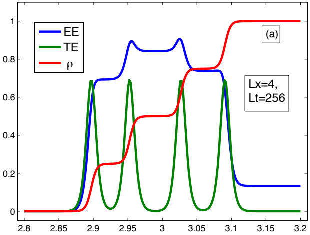

- Gauge invariant transfer matrix for the Abelian Higgs model in 1+1 dimensions (PRD 92 076003). This is an exact effective theory.
- Work in progress:
  - Central charge of $O(2)$ in the superfluid/KT phase (c=1?)
  - Polyakov loop in the abelian Higgs model (subtle at finite volume!)
  - Ising fermions (Grassmann version of the Kaufman solution; CFT?)
  - Numerical experiments for 2+1 $U(1)$ gauge theory on 4^3
- Schwinger model: Y. Shimizu and Y. Kuramashi ($\sim$ MPS work?)
- CP(N-1) models: H. Kawauchi and S.Takeda

The $O(2)$ model with a real chemical potential μ

$$Z = \int \prod_{(x,t)} \frac{d\theta_{(x,t)}}{2\pi} \mathrm{e}^{-S}.$$

$$\begin{aligned} S = & - \beta_\tau \sum_{(x,t)} \cos(\theta_{(x,t+1)} - \theta_{(x,t)} - i\mu) \\ & - \beta_s \sum_{(x,t)} \cos(\theta_{(x+1,t)} - \theta_{(x,t)}). \end{aligned}$$

$$\begin{aligned} Z &= \sum_{\{n\}} \prod_{(x,t)} I_{n_{(x,t),\hat{x}}}(\beta_s) I_{n_{(x,t),\hat{t}}}(\beta_\tau) e^{\mu n_{(x,t),\hat{t}}} \\ & \times \quad \delta_{n_{(x-1,t),\hat{x}}+n_{(x,t-1),\hat{t}}, n_{(x,t),\hat{x}}+n_{(x,t),\hat{t}}} \ . \end{aligned}$$

For real μ the action is complex, $\beta = 1/g^2$

Worm configurations

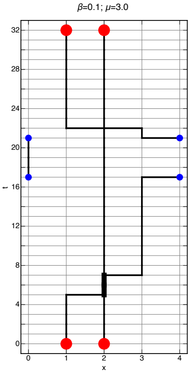

Figure: Allowed configuration of $\{n\}$ for a 4 by 32 lattice. The uncovered links on the grid have n=0, the more pronounced dark lines have $|n|$=1 and the wider lines have n=2. The dots need to be identified periodically. The time slice 5, represents a transition between $|1100\rangle$ and $|0200\rangle$. Statistical sampling of these configurations (worm algorithm, Banerjee and Chandrasekharan PRD 81) has been used to check the TRG calculations.

TRG approach of the transfer matrix

The partition function can be expressed in terms of a transfer matrix:

$$Z = \mathrm{Tr}\,\mathbb{T}^{L_t}\ .$$

The matrix elements of $\mathbb{T}$ can be expressed as a product of tensors associated with the sites of a time slice (fixed t) and traced over the space indices (PhysRevA.90.063603)

$$\mathbb{T}_{(n_1,n_2,\dots n_{L_x})(n'_1,n'_2\dots n'_{L_x})} = \sum_{\tilde{n}_1\tilde{n}_2\dots\tilde{n}_{L_x}} T^{(1,t)}_{\tilde{n}_{L_x}\tilde{n}_1 n_1 n'_1} T^{(2,t)}_{\tilde{n}_1\tilde{n}_2 n_2 n'_2\dots} \dots T^{(L_x,t)}_{\tilde{n}_{L_{x-1}}\tilde{n}_{L_x} n_{L_x} n'_{L_x}}$$

with

$$T^{(x,t)}_{\tilde{n}_{x-1}\tilde{n}_x n_x n'_x} = \sqrt{I_{n_x}(\beta_\tau) I_{n'_x}(\beta_\tau) I_{\tilde{n}_{x-1}}(\beta_s) I_{\tilde{n}_x}(\beta_s) \mathrm{e}^{(\mu(n_x+n'_x))}}\,\delta_{\tilde{n}_{x-1}+n_x,\tilde{n}_x+n'_x}$$

The Kronecker delta function reflects the existence of a conserved current, a good quantum number (“particle number").

Coarse-graining of the transfer matrix

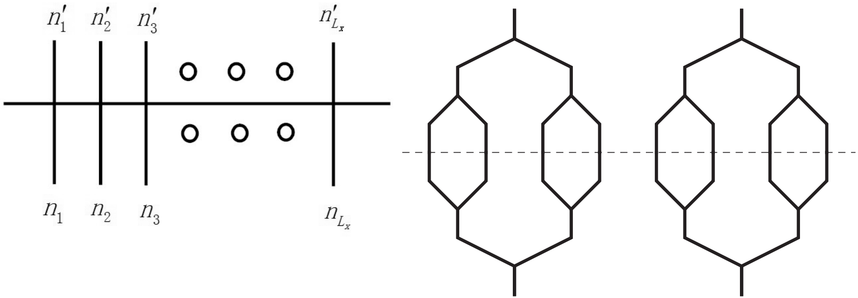

Figure: Graphical representation of the transfer matrix (left) and its successive coarse graining (right). See PRD 88 056005 and PRA 90, 063603 for explicit formulas.

Phase diagram

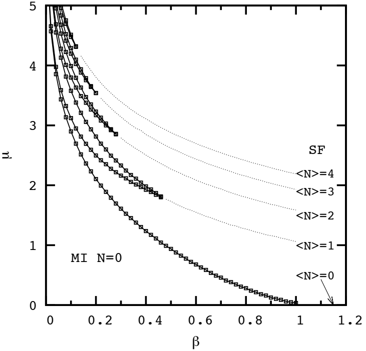

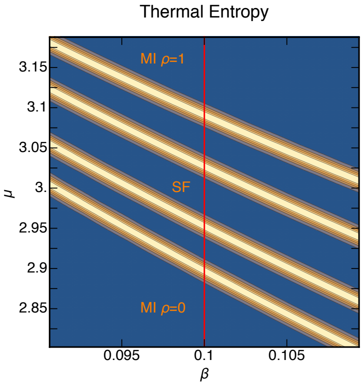

Figure: Mott Insulating “tongues" and Thermal entropy in a small region of the $\beta - \mu$ plane. Intensity plot for the thermal entropy of the classical XY model on a 4 $\times$ 128 lattice in the β-μ plane. The dark (blue) regions are close to zero and the light (yellow ochre) regions peak near $\ln 2$ (level crossing).

Entanglement entropy S_E (PRE 93, 012138 (2016))

We consider the subdivision of AB into A and B (two halves in our calculation) as a subdivision of the spatial indices.

$$\hat{\rho}_A \equiv \mathrm{Tr}_B \hat{\rho}_{AB}; \quad S_{EvonNeumann} = -\sum_i \rho_{A_i} \ln(\rho_{A_i}).$$

We use blocking methods until A and B are each reduced to a single site.

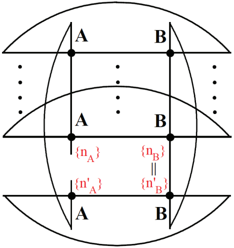

Figure: The horizontal lines represent the traces on the space indices. There are L_t of them, the missing ones being represented by dots. The two vertical lines represent the traces over the blocked time indices in A and B.

The fine structure of the EE for $N_s = 4$, $N_\tau = 256$

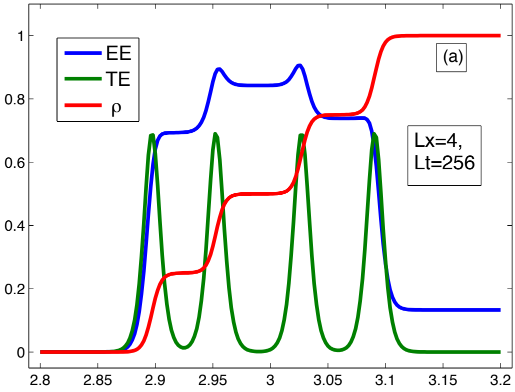

Figure: Entanglement entropy (EE, blue), thermal entropy (TE, green) and particle density ρ (red) versus the chemical potential μ . The thermal entropy has $N_s = 4$ peaks culminating near $\ln 2 \simeq 0.69$; ρ goes from 0 to 1 in $N_s = 4$ steps and the entanglement entropy has an approximate mirror symmetry near half fillings where it peaks.

Rényi entanglement entropy

The n -th order Rényi entanglement entropy is defined as:

$$S_n(A) \equiv \frac{1}{1-n} \ln(\mathrm{Tr}\,((\hat{\rho}_A)^n)) \ .$$

$\lim_{n\to 1^+} S_n$=von Neumann entanglement entropy.

The approximately linear behavior in $\ln(N_s)$ is consistent with the Calabrese-Cardy scaling which predicts

$$S_n(N_s) = K + \frac{c(n+1)}{6n} \ln(N_s)$$

for periodic boundary conditions and half the slope ($\frac{c(n+1)}{12n}$) for open boundary conditions. The constant K is non-universal and different in the four situations considered (n=1, 2 with PBC and OBC).

Time continuum limit

The time continuum limit can be achieved by increasing β_τ while keeping constant the products $\beta_s\beta_\tau = \tilde{J}/\tilde{U}$ and $\mu\beta_\tau = \tilde{\mu}/\tilde{U}$. This defines a rotor Hamiltonian:

$$\hat{H} = \frac{\tilde{U}}{2}\sum_x \hat{L}_x^2 - \tilde{\mu}\sum_x \hat{L}_x - \tilde{J}\sum_{\langle xy\rangle}\cos(\hat{\theta}_x - \hat{\theta}_y) \ ,$$

with $[\hat{L}_x, \mathrm{e}^{i\hat{\theta}_y}] = \delta_{xy}\mathrm{e}^{i\hat{\theta}_y}$. For quantum simulation purposes, these commutation relations can be approximated for finite integer spin. In the following we focus on the spin-1 approximation which can also be implemented in the classical system by setting the tensor elements to zero for space and time indices strictly larger then 1 in absolute value. The correspondence between the two methods can be checked with a Density Matrix Renormalization Group (DMRG) method which optimizes the entanglement entropy.

Rényi entanglement entropy, isotropic, $N_s = 4$, PBC

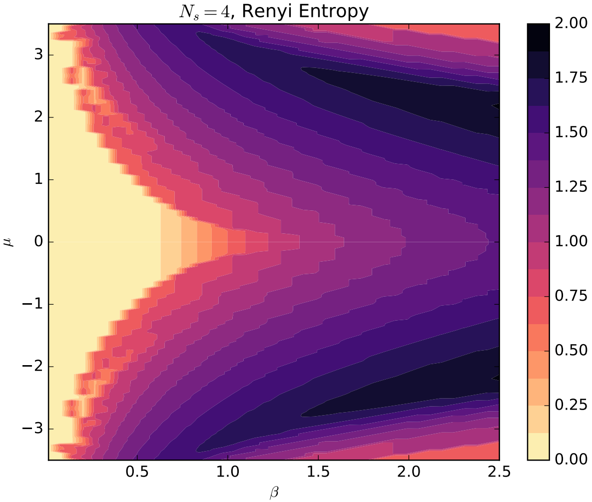

Figure: Picture made by Judah Unmuth-Yockey. Computational method developed with James Osborn at ANL.

Entanglement Entropies vs. ln(N_s), PBC and OBC

Case 1: half-occupancy in the superfluid phase phase.

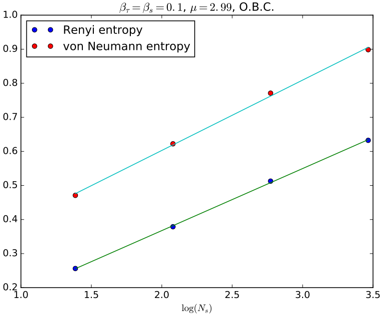

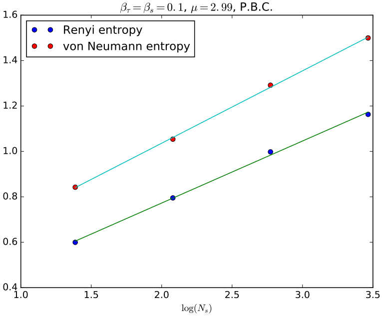

Entanglement Entropies vs. ln(N_s), continuous time

Case 1: half-occupancy in the superfluid phase phase. DMRG fits include one subleading correction (in progress).

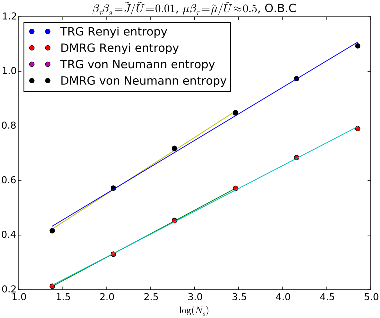

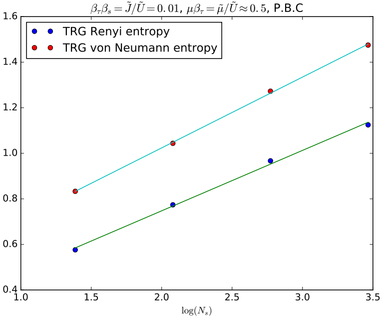

Entanglement Entropies vs. ln(N_s), PBC and OBC

Case 2: $\mu = 0$, $\beta \gg \beta_{KT}$

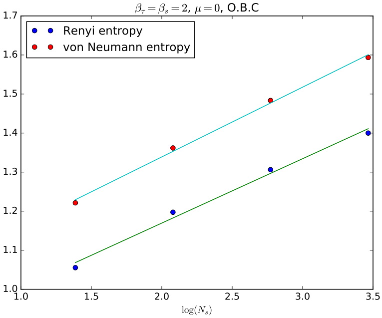

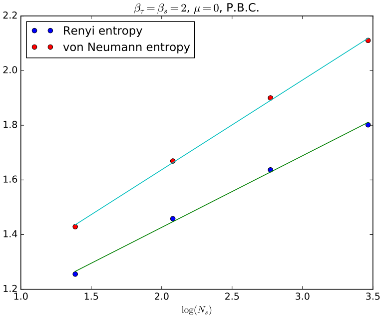

Entanglement Entropies vs. $\ln(N_s)$, continuous time

Case 2: $\mu = 0$, $\beta \gg \beta_{KT}$.
DMRG fits include one subleading correction.

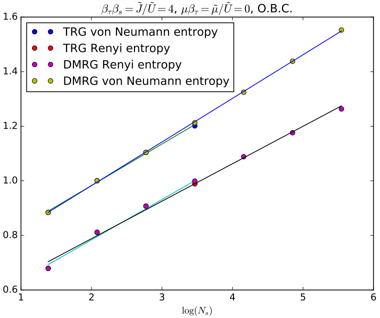

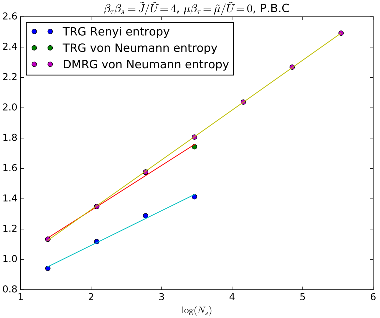

Preliminary slopes

In progress, subleading effects are small but not well understood ..

EE	isotropic	anisotropic	DMRG	$c = 1$ CFT
S_1 PBC	0.32(2)	0.31(2)	in progress	0.333...
S_2 PBC	0.27(2)	0.27(3)	in progress	0.25
S_1 OBC	0.20(2)	0.21(2)	in progress	0.166...
S_2 OBC	0.18(1)	0.17(1)	in progress	0.125

Table: Slopes of von Neumann and Renyi entropies for case 1.

EE	isotropic	anisotropic	DMRG	$c = 1$ CFT
S_1 PBC	0.33(2)	0.30(3)	0.328(4)	0.333...
S_2 PBC	0.26(3)	0.23(4)	in progress	0.25
S_1 OBC	0.18(2)	0.15(2)	0.159(1)	0.166...
S_2 OBC	0.16(4)	0.15(4)	0.14(1)	0.125

Table: Slopes of von Neumann and Renyi entropies for case 2.

Recent experiment (M. Greiner et al., Harvard)

Many-body interference to probe entanglement in optical lattices

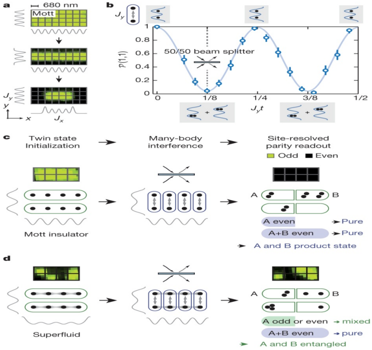

R Islam *et al.* *Nature* **528,** 79 (2015) doi:10.1038/nature15750

Recent experiment (M. Greiner et al. , Harvard)

Entanglement in the ground state of the Bose–Hubbard model

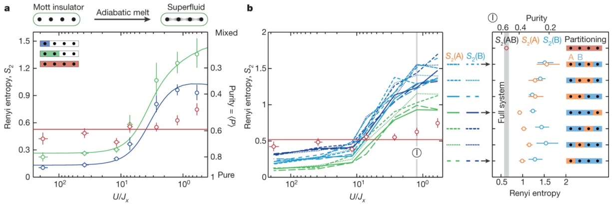

R Islam *et al. Nature* **528,** 80 (2015) doi:10.1038/nature15750

nature

The Abelian Higgs model on a 1+1 space-time lattice

a.k.a. lattice scalar electrodynamics. Field content:

- Complex (charged) scalar field $\phi_x = |\phi_x| \mathrm{e}^{i\theta_x}$ on space-time sites x
- Abelian gauge fields $U_{x,\mu} = \exp iA_\mu(x)$ on the links from x to $x + \hat{\mu}$
- $F_{\mu\nu}$ appears when taking products of U's around an elementary square (plaquette) in the $\mu\nu$ plane
- Notation for the plaquette: $U_{x,\mu\nu} = \mathrm{e}^{i(A(x)_\mu + A(x+\hat{\mu})_\nu - A(x+\hat{\nu})_\mu - A(x)_\nu)}$
- $\beta_{pl.} = 1/e^2$ and κ is the hopping coefficient

$$
\begin{aligned}
S &= -\beta_{pl.} \sum_x \sum_{\nu<\mu} \mathrm{Re}\mathrm{Tr}\left[U_{x,\mu\nu}\right] + \lambda \sum_x \left(\phi_x^\dagger \phi_x - 1\right)^2 + \sum_x \phi_x^\dagger \phi_x \\
&- \kappa \sum_x \sum_{\nu=1}^{d} \left[\mathrm{e}^{\mu_{ch.}\delta(\nu,t)} \phi_x^\dagger U_{x,\nu} \phi_{x+\hat{\nu}} + \mathrm{e}^{-\mu_{ch.}\delta(\nu,t)} \phi_{x+\hat{\nu}}^\dagger U_{x,\nu}^\dagger \phi_x\right].
\end{aligned}
$$

$$
Z = \int D\phi^\dagger D\phi D U e^{-S}
$$

Unlike other approaches (Reznik, Zohar, Cirac, Lewenstein, Kuno,....) we will not try to implement the gauge field on the optical lattice.

Tensor Renormalization Group formulation ($\lambda \to \infty$)

As in PRD.88.056005 and PRD.92.076003, we attach a $B^{(\square)}$ tensor to every plaquette

$$B^{(\square)}_{m_1 m_2 m_3 m_4} = \begin{cases} t_{m_\square}(\beta_{pl}), & \text{if } m_1 = m_2 = m_3 = m_4 = m_\square \\ 0, & \text{otherwise.} \end{cases}$$

a $A^{(s)}$ tensor to the horizontal links

$$A^{(s)}_{m_{up} m_{down}} = t_{|m_{down} - m_{up}|}(2\kappa_s),$$

and a $A^{(\tau)}$ tensor to the vertical links

$$A^{(\tau)}_{m_{left} m_{right}} = t_{|m_{left} - m_{right}|}(2\kappa_\tau)\, e^{\mu}.$$

The quantum numbers on the links are completely determined by the quantum numbers on the plaquettes

$Z = Tr[\prod T]$

$$Z = (I_0(\beta_{pl}) I_0(2\kappa_s) I_0(2\kappa_\tau))^V \times$$

$$\mathrm{Tr}\left[\prod_{h,v,\Box} A^{(s)}_{m_{up} m_{down}} A^{(\tau)}_{m_{right} m_{left}} B^{(\Box)}_{m_1 m_2 m_3 m_4}\right] \propto \mathrm{Tr}(\sqrt{\mathbb{B}}\mathbb{A}\sqrt{\mathbb{B}})^{N_\tau}.$$

The traces are performed by contracting the indices as shown

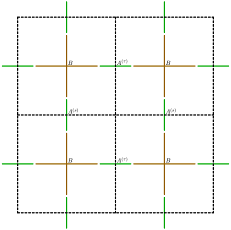

Figure: The basic B and A tensors (in brown and green, respectively, colors online). The $A^{(s)}$ are associated with the vertical tensors, and the horizontal (spatial) links of the lattice. The $A^{(\tau)}$ are associated with the horizontal tensors, and the vertical (temporal) links of the lattice.

Remarks

- The plaquette quantum numbers are the dual variables
- If we impose periodic boundary conditions on the plaquettes, we can only have neutral states (Gauss law)
- We will probe the charged sector by introducing Polyakov loops
- For related questions in QED, see arXiv:1509.01636, “Charged hadrons in local finite-volume QED+QCD with C* boundary conditions" by Biagio Lucini, Agostino Patella, Alberto Ramos, and Nazario Tantalo

Polyakov loop

Polyakov loop, a Wilson line wrapping around the Euclidean time direction: $\langle P_i \rangle = \langle \prod_j U_{(i,j),\tau} \rangle$; the order parameter for deconfinement.

With spatial periodic boundary condition, the insertion of the Polyakov loop (red) forces the presence of a scalar current (green) in the opposite direction (left) or another Polyakov loop (right).

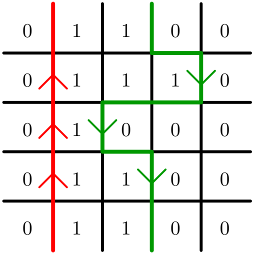

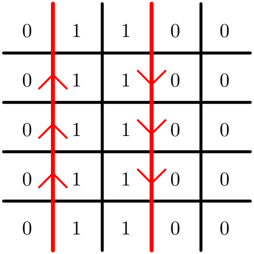

In the Hamiltonian formulation, we add $-\frac{\tilde{Y}}{2}(2(\bar{L}^z_{i^\star} - \bar{L}^z_{(i^\star+1)}) - 1)$ to H.

Polyakov loop: Numerical calculations

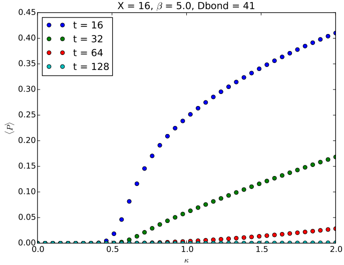

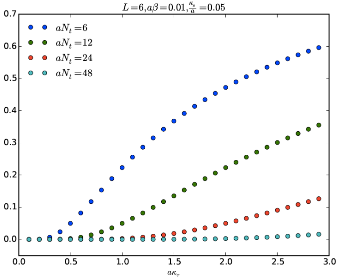

Polyakov loop for (1+1)D Abelian Higgs model using the TRG method (Left, Judah Unmuth-Yockey) and the Hamiltonian method (Right, Jin Zhang).

Data collapse for Polyakov loop

Guesses: $-\ln(P) \simeq C + N_\tau(\Delta E)$; $\Delta E \simeq A/N_s + Bg^2 N_s + ...)$;
Data Collapse: $N_s \Delta E = F(g^2 N_s^2)$?
Recent numerical calculations by J. Unmuth-Yockey give support to this idea

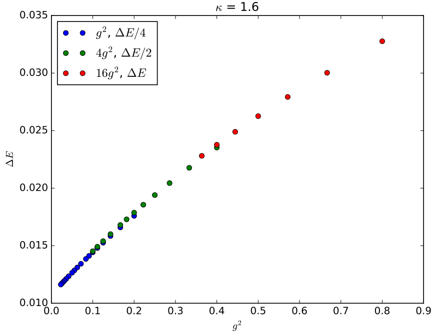

Data collapse for Polyakov loop II

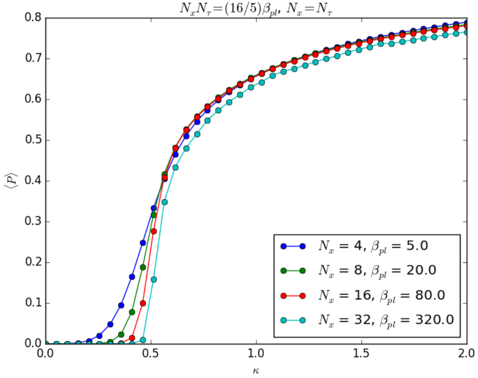

Figure: The increase in sharpness with volume makes it look like an order parameter. Numerical calculations by J. Unmuth-Yockey.

Can lattice gauge theorists learn about Quantum Chromodynamics (QCD) at finite density and real time from optical lattice experiments?

The Fermilab Lattice Gauge Theory cluster (left); An optical lattice experiment (once used to observe a “Higgs mode") at MPQ (right)

Quantum Simulators

- No sign problems
- Real time evolution
- So far the linear sizes are of order 100-200 and are expected to reach 1000 soon.
- Finite temperature at infinite size (Euclidean time)$\sim$ finite size at zero temperature (experiment)?
- Many interesting proposals based on the Kogut-Susskind Hamiltonian and quantum rotors (Reznik, Zohar, Cirac, Wiese, Lewenstein, Kuno,....).
- Black holes? (Masanori Hanada, this conference).
- Our approach is based on the tensor formulation of lattice gauge theory and is manifestly gauge invariant.
- So far, the remarkable theory-experiment reached for the Bose-Hubbard model is just a source of inspiration in the context of lattice gauge theory and a proof of principle is needed.

Conclusions

- The tensor renormalization group formulation allows reliable calculations of the phase diagram and spectrum of the 1+1 D $O(2)$ model with a chemical potential.
- Calculations of the von Neumann and Rényi entanglement entropy for the $O(2)$ model in the superfluid phase at increasing N_s seem consistent with a CFT of central charge 1.
- Subleading corrections to Calabrese-Cardy scaling are small (but not well understood): measurements using cold atoms?
- Truncation errors need to be understood better.
- We have proposed a gauge-invariant approach for the quantum simulation of the abelian Higgs model.
- Calculations of the Polyakov loop at finite N_s and small gauge coupling shows an interesting behavior. Nice data collapse at weak gauge coupling.
- Thanks!

3D gauge theories

A blocking procedure can be constructed by sequentially combining two cubes into one in each of the directions (PRD 88 056005)

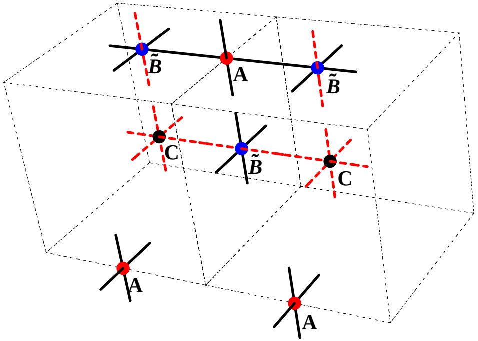

Quantum simulators: main message

- We have reformulated the lattice Abelian Higgs model (scalar QED) in 1 space + 1 time dimension using the Tensor Renormalization Group method
- The reformulation is gauge invariant and connects smoothly the classical Lagrangian formulation used by lattice gauge theorists and the quantum Hamiltonian method used in condensed matter
- Despite its simplicity, the model has a rich behavior (entanglement entropy scaling like in Conformal Field Theory in the weak gauge coupling limit, deconfinement at finite volume)
- We propose to use Bose-Hubbard (BH) Hamiltonians with two species as quantum simulators. Using degenerate perturbation theory, we obtain effective Hamiltonians resembling those relevant for the Abelian Higgs model
- We would like to find realistic ways to implement these BH Hamiltonians on optical lattices

The (high) standards: Quantum Monte Carlo vs. Experiment for the Bose-Hubbard model

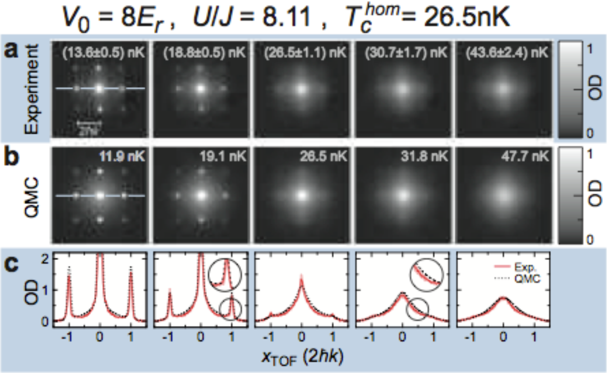

Figure: From S. Trotzky, L. Pollet, F. Gerbier, U. Schnorrberger, I. Bloch, N.V. Prokof'ev, B. Svistunov, M. Troyer Nature Phys. 6, 998-1004 (2010)

Two species Bose-Hubbard (PRD 92 076003)

The two-species Bose-Hubbard Hamiltonian ($\alpha = a, b$ indicates two different species, respectively) on square optical lattice reads

$$
\begin{aligned}
\mathcal{H} &= -\sum_{\langle ij \rangle}(t_a a_i^\dagger a_j + t_b b_i^\dagger b_j + h.c.) - \sum_{i,\alpha}(\mu + \Delta_\alpha) n_i^\alpha \\
&+ \sum_{i,\alpha} \frac{U_\alpha}{2} n_i^\alpha (n_i^\alpha - 1) + W \sum_i n_i^a n_i^b + \sum_{\langle ij \rangle \alpha} V_\alpha n_i^\alpha n_j^\alpha \\
&- (t_{ab}/2) \sum_i (a_i^\dagger b_i + b_i^\dagger a_i)
\end{aligned}
$$

with $n_i^a = a_i^\dagger a_i$ and $n_i^b = b_i^\dagger b_i$.
In the limit where $U_a = U_b = U$ and W and $\mu_{a+b} = (3/2)U$ much larger than any other energy scale, we have the condition $n_i^a + n_i^b = 2$ for the low energy sector. The three states $|2, 0\rangle$, $|1, 1\rangle$ and $|0, 2\rangle$ satisfy this condition and correspond to the three states of the spin-1 projection considered above.

Using degenerate perturbation theory

$$
\begin{aligned}
\mathcal{H}_{eff} &= \left(\frac{V_a}{2} - \frac{t_a^2}{U_0} + \frac{V_b}{2} - \frac{t_b^2}{U_0}\right)\sum_{\langle ij\rangle} L_i^z L_j^z \\
&+ \frac{-t_a t_b}{U_0}\sum_{\langle ij\rangle}(L_i^+ L_j^- + L_i^- L_j^+) + (U_0 - W)\sum_i (L_i^z)^2 \\
&+ \left[\left(\frac{pn}{2}V_a + \Delta_a - \frac{p(n+1)t_a^2}{U_0}\right) - \left(\frac{pn}{2}V_b\right.\right. \\
&+ \left.\left.\Delta_b - \frac{p(n+1)t_b^2}{U_0}\right)\right]\sum_i L_i^z - t_{ab}\sum_i L_{(i)}^x
\end{aligned}
$$

where p is the number of neighbors and n is the occupation ($p = 2$, $n = 2$ in the case under consideration). $\hat{L}$ is the angular momentum operator in representation $n/2$.

Matching the O(2) and BH spectra for large U

Matching: with the $O(2)$ model, we need to tune the hopping amplitude as $t_\alpha = \sqrt{V_\alpha U/2}$ and have $\tilde{J} = 4\sqrt{V_a V_b}$, $\tilde{U} = 2(U - W)$, and $\tilde{\mu} = -(\Delta_a - V_a) + (\Delta_b - V_b)$.

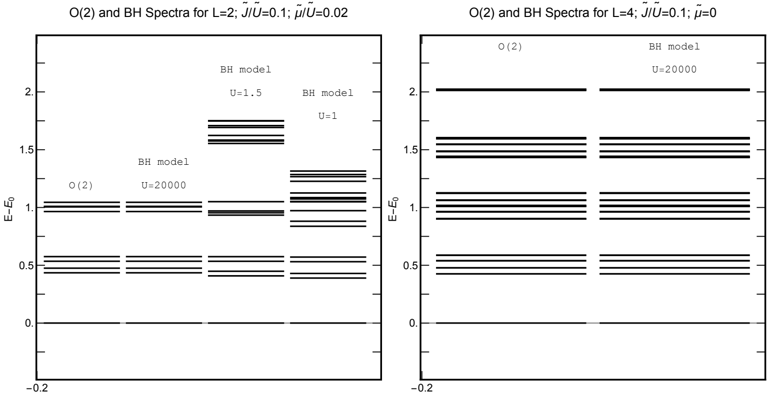

Figure: O(2) and Bose-Hubbard spectra for L=2 (left) and L=4 (right).

Optical lattice implementation (PRA 90 06303)

- The two-species: ^{87}Rb and ^{41}K Bose-Bose mixture where an interspecies Feshbach resonance is accessible (W).
- Species-dependent optical lattice are used in boson systems, which allows hopping amplitude of individual species to be tuned to desired values.
- The extended repulsion, V_α, is present and small when we consider Wannier gaussian wave functions sitting on nearby lattice sites (Mazzarella et al. 2006)

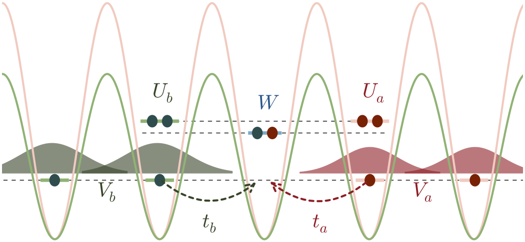

Matching Abelian Higgs model and BH spectra

$$\text{Matching: } t_a = t_b = 0,\ V_a = V_b = -\tilde{Y}/2,\ t_{ab} = \tilde{X},$$
$$\tilde{U}_p = 2(U - W + 2V_{a(b)}),\ \Delta_{a(b)} = -2V_{a(b)}.$$

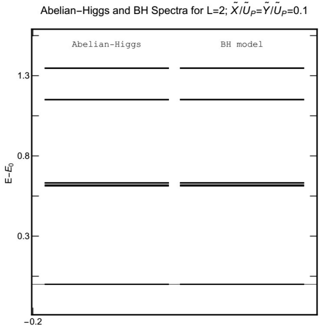

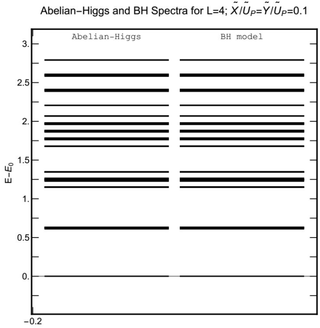

Optical lattice implementation

- Ladder structure

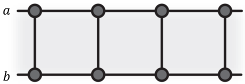

Figure: A ladder structure with a and b corresponding to the two sides of the ladder (right).

- Two species -> hyperfine states?
- Polar molecules?

QCD with chemical potential on $S_1 \times S_3$

QCD at finite chemical potential in a small hyperspherical box — Joyce C. Myers

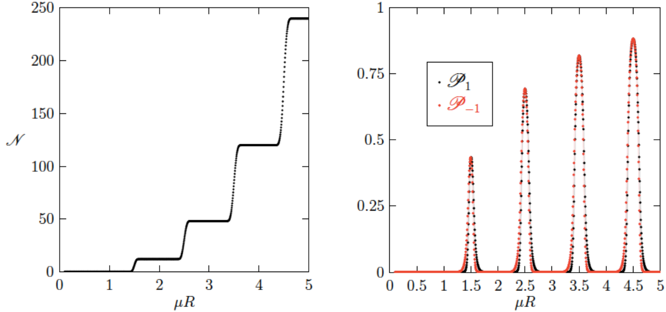

Figure 1: Quark number (Left) and Polyakov lines (Right) as a function of the chemical potential for QCD on $S^1 \times S^3$. (Right). $N = 3, N_f = 1, m = 0, \beta/R = 30$ (low T).

Figure: From: Simon Hands, Timothy J. Hollowood, Joyce C. Myers, arxiv 1012.0192, Lattice 2010.

Combining TRG and new perturbative methods?

- The divergence of QFT perturbative series can be traced to the large field configurations. For suitably chosen field cuts, converging perturbative series provide good approximation of results that can be obtained by independent numerical methods. The method can be combined with blocking for the hierarchical model. (YM, PRL 88, 141601 (2002)).
- In many of the TRG calculations, the microscopic tensor is constructed in terms of $I_n(\beta) = \frac{1}{2\pi}\int_{-\pi}^{\pi} d\theta \mathrm{e}^{\beta\cos(\theta)+in\theta}$. In the known asymptotic expansions of the $I_n(\beta)$, one adds tails of integration to the compact range in order to get Gaussian integrals. Keeping the range of integration finite leads to converging weak coupling expansion (L. Li and YM PRD 71 054509 (2005)). Hopefully this can be connected to resurgence ideas.
- Understanding the connection between topology and the perturbative expansion for the 1D O(2) model on a lattice is easy (Poisson summation), but a challenging problem in 2D.